Review

Hydrochemical and isotopical evidence of ground water salinization processes on the coastal plain of Samborombón Bay, Argentina

Eleonora Carol [a], Eduardo Kruse [a,*], Josep Mas-Pla [b]

[a] Consejo Nacional de Investigaciones Científicas y Técnicas (CONICET), Facultad de Ciencias Naturales y Museo, Universidad Nacional de La Plata (UNLP), Calle 64 #3 (entre 119 y 120), 1900, La Plata, Buenos Aires, Argentina
[b] Centre de Geologia i Cartografia Ambientals (GEOCAMB), Àrea de Geodinàmica, Dept. de Ciències Ambientals, Universitat de Girona, Campus de Montilivi, 17071, Girona, Spain

ARTICLE INFO

SUMMARY

Salinization in coastal areas of the province of Buenos Aires, Argentina, is a controlling factor of water quality, and limits its exploitation for human uses and local ecological values. Coastal plains such as the one in the southern part of Samborombón Bay have a tidal morphology consisting of fine sediment deposits, tidal channels, and aeolian sand sheets, each of them playing a hydrological role. In this paper, we describe the hydrological processes in the Samborombón Bay coastal plain using hydrochemical and isotopical data to provide evidence of salinization processes. Specific ionic relationships for surface and ground water samples from each formation are differ from those of sea water. Isotopic data also reveal infrequent participation of sea water in the coastal area water samples, showing an evaporation trend in both surface and ground water. We conclude that salinization has its origin in the occurrence of gypsum and halite, as well as other chlorides, from the coastal plain deposits. Rainfall recharge, continental water inputs, evaporation and long residence times define the hydrochemical and isotopical features of ground water, which shows no signs of present sea water contribution. Sand sheets constitute local aquifers with lower salinity content. Continental surface waters, as well as rainfall drainage via tidal channels, have a dominant effect on surface water hydrochemistry notwithstanding tidal oscillations. Exploitation of water resources is thus limited to regionally extended aeolian sand sheet formations and to surface waters, specifically those related to contributions of freshwater discharge from inland areas.

© 2008 Elsevier B.V. All rights reserved.

Contents

* Corresponding author. Tel.: +54 221 4249049; fax: +54 221 4841383.
  E-mail addresses: eleocarol@fcnym.unlp.edu.ar (E. Carol), kruse@fcaglp.unlp.edu.ar (E. Kruse).

Introduction

The eastern and north-eastern coasts of the province of Buenos Aires (Argentina) possess a wide coastal plain where ecological val-

ues, as well as economic development, depend on fresh water availability in a saline dominated environment. Existing water supply systems and economic activity, mainly cattle rearing, rely on traditional methods of ground water exploitation with no thorough
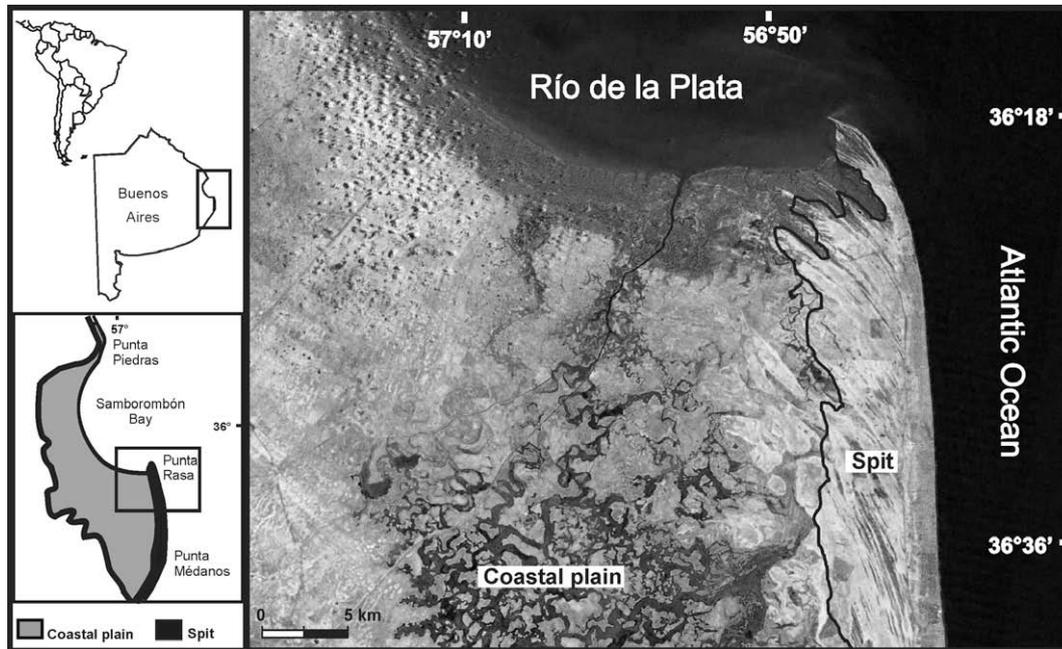

Fig. 1. Geographic location and aerial view of the study area.
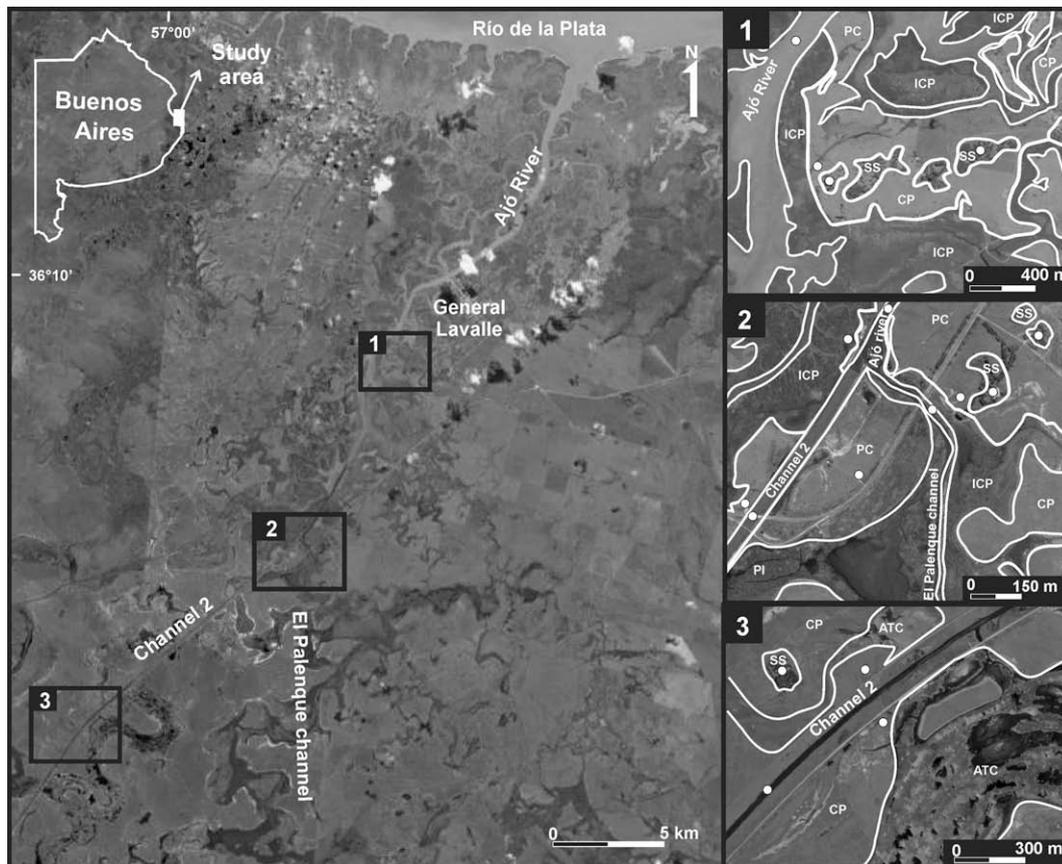

Fig. 2. Location of the different selected sites within the Samborombón Bay coastal plain. Surface and ground water sampling points are represented by dots. Geomorphological features of each site are also mapped as follows; PC: coastal plain, PI: intertidal coastal plain, ACM: ancient tidal channels, and MA: aeolian sand sheets.
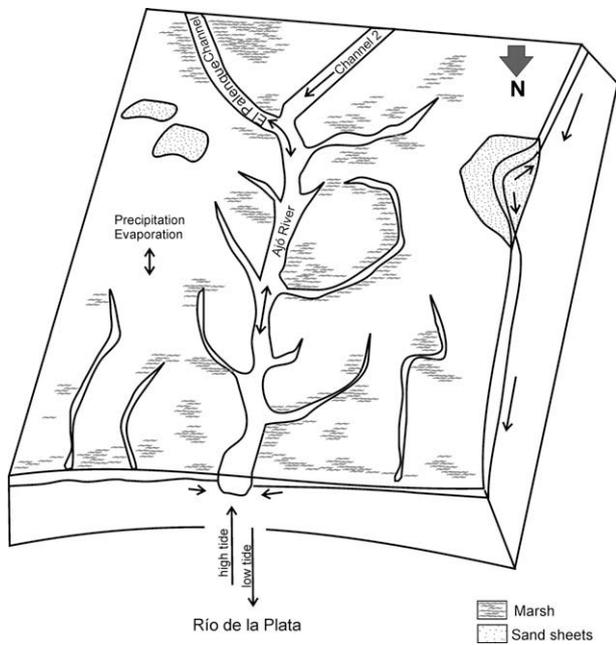
Fig. 3. Hydrological scheme of the Samborombón Bay coastal plain.

evaluation of hydrological possibilities. Intensive development may lead, therefore, to unnecessary alterations in the fragile hydro-morphological and ecological balance.

The coastal plain of Samborombón Bay was developed over several transgressive periods during the Quaternary. Its morphology reveals the joint influence of tidal dynamics upon sediment input from mainland rivers and coastal transport. Sedimentary features determine the hydrogeological as well as hydrochemical processes in these areas, which have been poorly investigated as they are periodically flooded over long time spans. Such hydrological processes play a significant role in the equilibrium of regional ecosystems. In particular, most of these areas are defined as natural reserves whose future preservation and management largely depends on appropriate knowledge of their specific hydrological features.

These coastal wetlands and plains are thus complex hydrogeological areas, with the usual occurrence of shallow saline ground water. Salinity can be attributed to many origins, such as marine contribution (Groen et al., 2000; Jorgensen, 2002; Kim et al., 2003), the dissolution of secondary minerals within the sedimentary formations (Howard and Lloyd, 1983), evaporation of sea water (Robinson and Gunatilaka, 1991), transpiration by mangrove vegetation (Fass et al., 2007), flow of saline water from the adjacent aquifer, return flow from irrigation water, anthropogenic contamination, or most often, a combination of some of these processes (Kamel et al., 2005; Marimuthu et al., 2005; Park et al., 2005; Ghabayen et al., 2006; Djabri et al., 2008; El Mandour et al., 2008).

The particular hydrogeology of the province of Buenos Aires coastal plains has been studied from a regional perspective by Sala et al. (1978), Ainchil et al. (2004), Kruse et al. (2005), Carol et al. (2008); and from a more local one by Logan and Rudolph (1997), Logan and Nicholson (1998) and Logan et al. (1999). These authors demonstrate the hydrological characteristics of the coastal plains, specifically their low hydraulic conductivity, and that ground water usually shows a high salinity content.

The objective of the present work is to investigate the hydrological dynamics of these coastal plain areas, and specifically those of the southern part of Samborombón Bay, based on hydrochemical and isotopical data. Our aim is to describe the salinization

Table 1
Hydrochemical data from surface and ground water. S1, S2, and S3 in the sample name refer to Sites #1, #2, and #3, respectively.

| | Sample | EC (µS/cm) | TDS (mg/L) | pH | HCO$_3^-$ (meq/L) | CO$_3^{2-}$ (meq/L) | SO$_4^{2-}$ (meq/L) | Cl$^-$ (meq/L) | Ca^{2+} (meq/L) | Mg^{2+} (meq/L) | Na$^+$ (meq/L) | K$^+$ (meq/L) | p CO$_2$ (atm) | Saturation index | | |
														Calcite	Gypsum	Halite
Groundwater																
Coastal plain	CP1 S1	38 000	25 600	7.2	16.06	0.00	33.31	370.52	89.82	20.98	318.62	5.11	4.5×10^{-3}	1.35	-0.1	-2.81
	CP2 S2	20 800	13 525	6.6	9.80	0.00	17.01	190.27	25.95	37.02	146.19	3.66	13×10^{-2}	0.13	-0.72	-3.40
	CP3 S2	5 130	3 200	7.6	24.79	0.00	5.45	24.82	2.19	2.09	50.02	0.89	4.2×10^{-3}	0.65	-1.82	-4.65
	CP4 S2	30 400	19 465	7.8	19.60	0.00	23.74	270.38	19.96	52.98	238.15	3.96	1.4×10^{-3}	1.42	-0.81	-3.06
	CP5 S2	44 000	30 795	7.1	18.60	0.00	67.69	424.60	95.81	39.98	364.29	6.01	6.2×10^{-3}	1.30	0.16	-2.70
	CP6 S3	17 600	10 985	7.3	14.60	0.00	17.61	154.22	23.95	18.02	139.19	2.92	4.0×10^{-3}	0.98	-0.67	-3.50
	CP7 S3	19 000	11 950	7.5	21.09	0.00	26.44	158.22	19.96	19.99	149.16	2.30	3.6×10^{-3}	1.22	-0.60	-3.47
Sand sheet	SS1 S1	5 430	3 140	7.3	11.60	0.00	3.27	40.06	10.88	2.60	38.15	4.14	3.8×10^{-3}	0.76	-1.35	-4.57
	SS2 S1	2 500	1 670	7.5	12.09	0.00	2.64	10.21	4.79	0.90	17.83	1.59	2.7×10^{-3}	0.72	-1.60	-5.44
	SS3 S2	5 850	3 725	7.7	10.80	0.00	2.31	45.67	18.96	0.49	43.50	2.25	1.3×10^{-3}	1.34	-1.31	-4.46
	SS4 S2	19 600	13 850	7.0	11.09	0.00	41.58	162.23	71.86	14.97	122.66	8.18	5.7×10^{-3}	0.97	0.06	-3.55
	SS5 S3	26 300	18 430	7.1	16.60	0.00	50.38	228.32	59.88	50.02	174.42	6.75	6.3×10^{-3}	1.11	-0.04	-3.27
Surface water																
Channel 2	C2 S2	962	575	7.9	2.56	0.00	1.64	4.71	1.99	0.59	6.17	0.31	2.4×10^{-3}	0.20	-1.95	-6.19
	C2 S3	2 290	1 315	8.3	5.49	0.18	4.66	12.33	6.19	0.90	15.66	0.46	1.8×10^{-3}	1.26	-1.24	-5.41
El Palenque Channel	EP S2	2 590	1 495	7.6	2.93	0.00	4.08	17.24	6.99	0.81	16.88	0.74	5.4×10^{-3}	0.38	-1.24	-5.24
Ajó River	R S1	6 730	4 345	7.7	2.82	0.00	6.91	60.08	5.79	10.12	51.76	1.48	3.6×10^{-3}	0.24	-1.36	-4.27
	R S2	2 360	1 345	7.7	2.91	0.00	4.08	15.31	6.58	0.80	15.48	0.69	4.1×10^{-3}	0.46	-1.25	-5.33

processes that influence ground water quality and restrict it for human uses. Such knowledge will contribute to adequate land and water planning strategies, as well as to preventing quantitative and qualitative alteration of the environmental conditions.

Geographical and geological setting

Samborombón Bay is located in the east of the province Buenos Aires, Argentina. The southern coast of the bay consists of a transitional area between the furthest zone influenced by the Rio de la Plata, and the Atlantic Ocean. Coastal mixing processes determine the environmental characteristics of the bay. We pay particular attention to a large coastal plain (ca. 3000 km^2) that was formed during the Pleistocene and Holocene under similar geomorphological conditions as today. Its origin is related to the northward migration by littoral drift of a large sandy spit, 70 km long and 9 km wide, from Punta Médanos to Punta Rasa. This beach and dune formation, jointly with the tidal dynamics of the Atlantic Ocean, provided adequate conditions for the growth of an extensive marsh and tidal coast plain on the western side of the bay (Violante and Parker, 2000; Violante et al., 2001). The study area lies in the southern sector, along a 25 km coastline, with a width of 30 km (Fig. 1).

The coastal plain has a regional slope of 10^{-5} m/m towards the north, with an average altitude of 1.6 m above sea level. Outcropping materials consist of silt and clay sediments related to marine environments, in which interbedded layers with abundant shells or gypsum are commonly found (Parker, 1979). Above the fine sediment formations, recent sandy sheets of aeolian origin form a patch of relatively elevated (2.5 m a.s.l.) mounds of reduced dimensions.

The regional climate is classified as subhumid–humid, mesothermal, with scarce or even nil water deficiency (Thornthwaite, 1948). Mean annual rainfall reaches 930 mm, and the average temperature is 14.6 °C. Potential evapotranspiration is 770 mm per year, according to the Thornthwaite and Mather (1955) method.

Methodology

Sampling points for surface and ground water investigation were based on geological and geomorphological information obtained on the field, and a detailed observation of satellite images and topographic maps.

Three distinct sites, each of them representative of the distinct environments on the coastal plain (Fig. 2), were differentiated to provide an integrated view of the hydrological processes in the Samborombón Bay coastal plain. Site 1 represents the influence of estuarine water inputs through the Ajó River, a major tidal channel within the coastal plain; Site 2 investigates the effect of El Palenque channel on the drainage of the coastal marshes; and finally, Site 3 was selected as being near to Channel 2, which artificially brings fresh surface water inputs inside the coastal plain. In this paper, we deal with the data set collected on September 2005 (Carol, 2008).

Samples were obtained through manually drilled boreholes to depths of 3 m. Physico-chemical parameters, such as electrical conductivity (EC) and pH (both measured in the field), as well as major ions (HCO_3^-, CO_3^{2-}, SO_4^{2-}, Cl^-, NO_3^-, Ca^{2+}, Mg^{2+}, Na^+, K^+), were analysed for surface and ground water samples. Environmental water isotopes, like oxygen 18 and deuterium, were also measured. Chemical analyses were conducted at the Laboratorio de Ingeniería
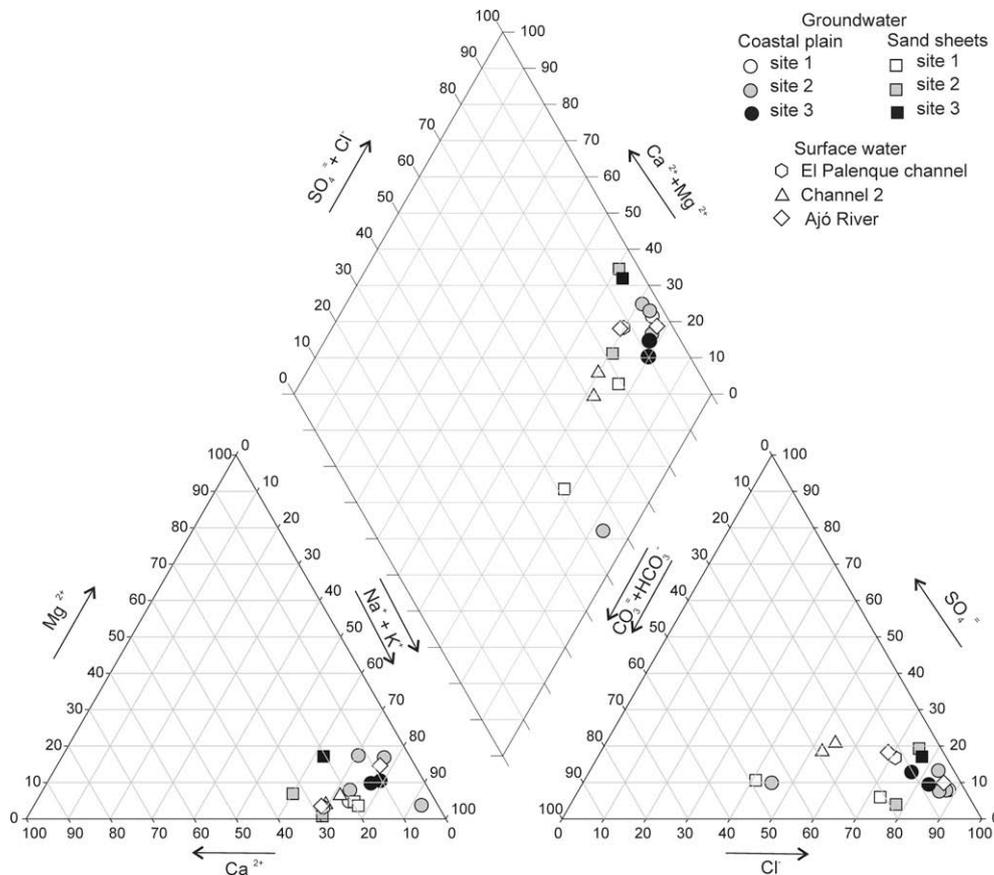

Fig. 4. Piper diagram of surface and ground water samples.

Sanitaria, Facultad de Ingeniería, Universidad Nacional de La Plata. Sample collection, preservation and analysis were performed in accordance with the American Public Health Association (APHA, 1998). Ionic speciation, partial pressure of CO_2, and saturation indices were estimated using PHREEQC 2.13 (Parkhurst and Appelo, 1999). Reference values for sea water are those by Stumm and Morgan (1981).

Isotopical analysis of $\delta^{18}O$ and δD were conducted at the Instituto de Geocronología y Geología Isotópica, Buenos Aires. Isotopical relations were measured in accordance with Coleman et al. (1982) and Panarello and Paricia (1984), using a Finnigan MAT Delta S mass-spectrometer with triple collector and multiple induction system. Results, expressed as isotopic deviation δ (‰), were

$$\delta = 1000 \cdot \frac{Rs - Rp}{Rp},$$

where Rs is the isotopic relation ($^2H/^1H$, $^{18}O/^{16}O$) of the simple and Rp the isotopic relation of the international standard reference. Standards used are the Vienna Standard Mean Ocean Water (V-SMOW) (Gonfiantini, 1978). Analytical uncertainties are of ±0.2 for $\delta^{18}O$, and ±0.1 for δD.

Results

Geomorphology

The coastal plain consists of two main geomorphological environments of hydrological significance: firstly, the tidal coastal plain with an occurrence of ancient and recent tidal channels; and secondly, occasional sand sheets of low elevation (Figs. 2 and 3).

The gentle-slope tidal coastal plain consists of silt and clay sediments associated with type soils as natraquert and cromic salaquent (Soil Taxonomy, 1999). Those are poorly drained soils, with low to moderate hydraulic conductitivy, alkaline, saline a mottled pattern of colours related to the occurrence of iron and manganese as a result of soils hydromorphics. It shows a transitional boundary with the intertidal area, and also with surface water stream channels, with levees 0.5 m high. Ancient tidal channels can be recognised in most of the continental areas that are currently disconnected from tidal oscillation.

The intertidal plain is well developed along the margins of the Ajó River and El Palenque channel and other minor tidal channels, and is daily flooded at high tide. Elevation in this area is below 1.10 m a.s.l. and has almost no slope towards the channels. Terrains are mainly
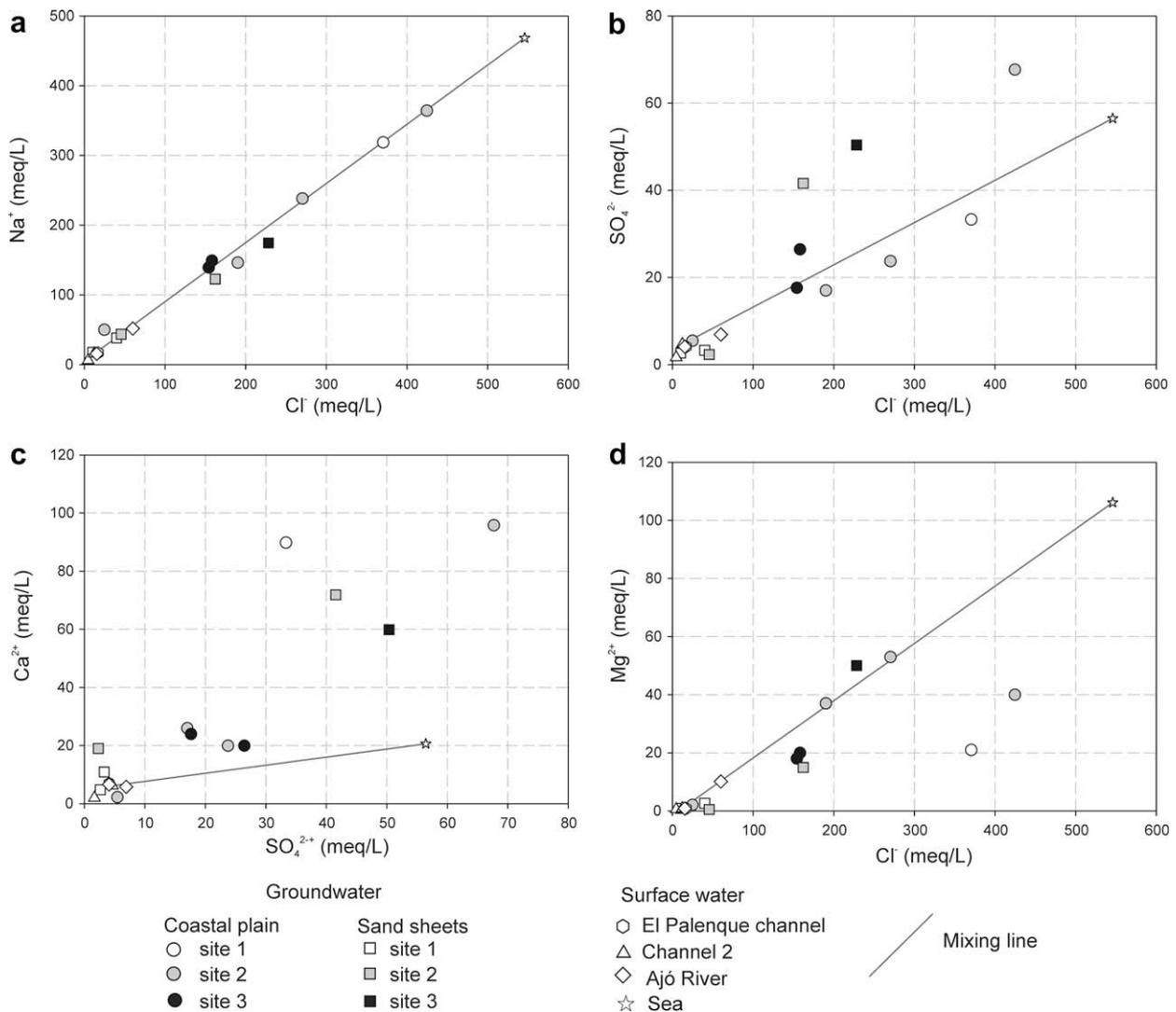

Fig. 5. Hydrochemical relationships between selected ions of surface and ground water samples and sea water mean composition, as given by Stumm and Morgan (1981). Mixing line between sea water and surface water from Channel 2 at Site #3 is plotted for reference. Dots on the line represent mixing proportions of 10% increments.

constituted by silt and clay sediments, with type soils as natraquert and undiffered (Soil Taxonomy, 1999), being similar to those of the coastal, yet they can be temporally flooded.

Aeolian sandy sheets are only found occasionally on the coastal plain. They have distinct morphologies, normally a reduced area (usually less than 0.1 km², and elevations about 2.5 m above the plain. Lithologically, the sand sheets are constituted by fine sand with fragments of shells, forming well drained deposits. Soil types are defined as thapto natric hapludoll and typic natraquert (Soil Taxonomy, 1999), with very low salinity and no signs of hydromorphism. Each sand sheet stores a limited amount of ground water with specific hydrodynamic and hydrochemical properties (Carol et al., 2008).

Hydrology

Flow discharge in the area is towards Samborombón Bay, in the Rio de la Plata, and mainly takes place through surface runoff. The Ajó River flows into the Bay, with contributions from the El Palenque channel and Channel 2 (Fig. 3).

Samborombón Bay has a microtidal regime, with a tidal amplitude of less than 2 m. At high tide, water floods the coastal plain through tidal channels and the Ajó River, affecting an area 20 km wide as a result of the low topographic gradient of the plain. The influence of high tide also reaches the El Palenque channel, but it does not affect Channel 2 as a dam has been built to protect it from tidal events.

Potentiometric data suggests that ground water flows in a north-eastern direction; although a hydraulic gradient less than 10^{-5} m/m and an expected low hydraulic conductivity in the coastal plain materials indicate that the overall continental subsurface discharge to the bay is negligible. Main ground water discharge occurs towards the tidal channels, specifically to the Ajó River and related minor drains. Temporal variations in the flow direction have been observed near these channels, related to the bank-storage changes caused by tidal oscillations.

Rainfall events recharge the unconfined aquifer levels in the coastal plain, and because of the proximity of the water table, ponds are likely to appear all across the plain. In the water balance, potential evapotranspiration occurs as the water table is located at root depth. Potential evapotranspiration rates larger than 100 mm per month are recorded between December and February, altogether with a lowering of the water table. The lowest evapotranspiration values occur in the winter season, from June to August, with values lower than 30 mm per month, and with water table levels close to the soil surface. Aeolian sand sheets play, therefore a distinct role in ground water dynamics based on their high hydraulic conductivity, and its bounded geometry by less permeable lithologies. Nevertheless, their relative altitude above the plain allows ground water storage and controls recharge flow rate towards the plain.

Hydrochemistry

Ground water hydrochemistry

Ground water in the coastal plain presents sodium–chloride facies, with a high salinity content ranking from total dissolved solid values of 3200–30 795 mg/L, with sulphate content similar to that
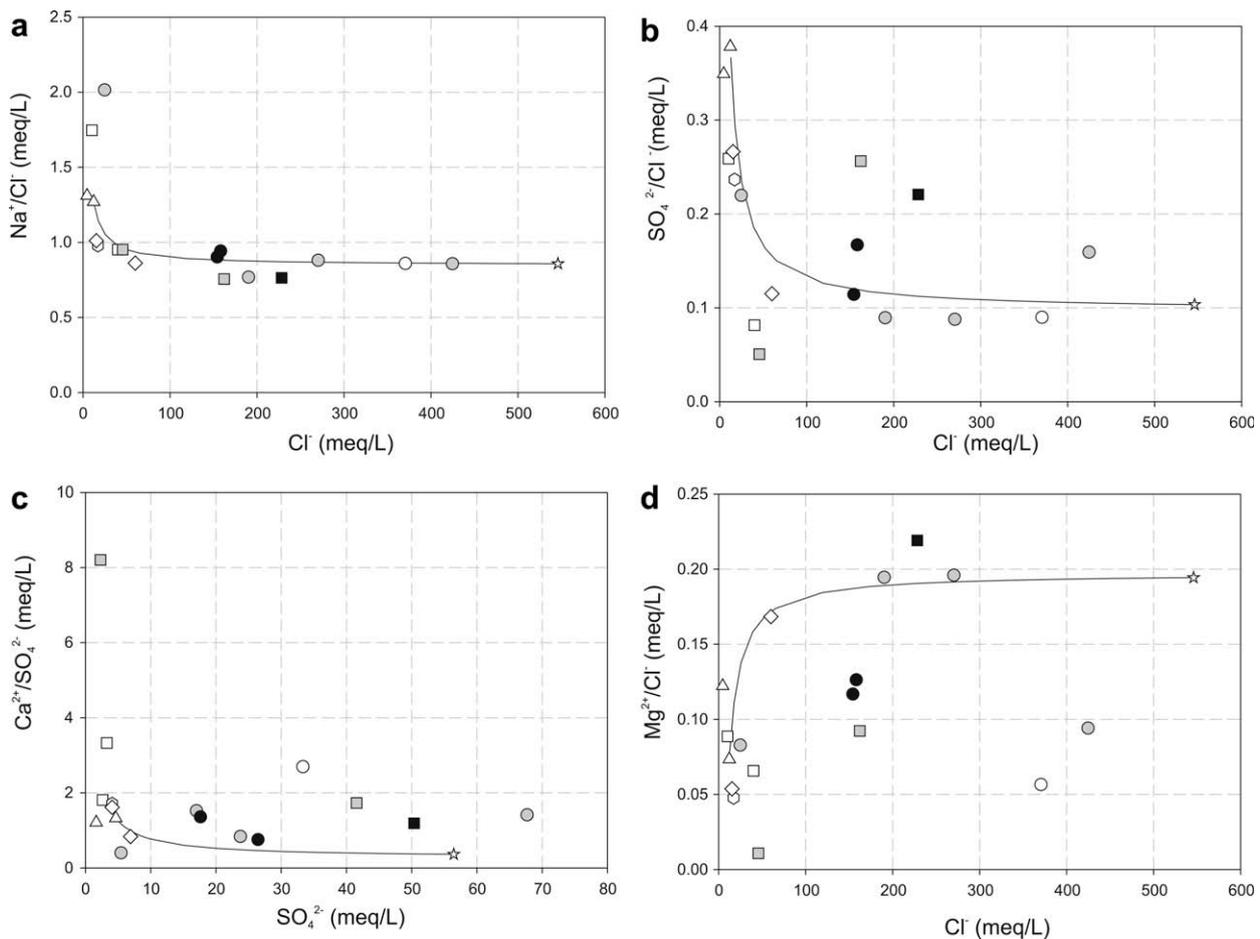

Fig. 6. Evolution of some hydrochemical ratios with increasing salinity, and their correspondence to sea water. Legend and mixing line as in Fig. 5.

of bicarbonate when given in meq/L. Distinctively, sand sheets may present sodium–chloride facies, with salinity contents between 1670 and 18 430 mg/L depending on the interbedding with coastal plain deposits (Table 1, Fig. 4). In sand sheets, alkalinity values, expressed as HCO_3^-, are larger than those of sulphate (except for two samples) as a sign of the distinct soil-mineral content of both sedimentary formations.

In particular, sodium increases linearly with chloride (Fig. 5a). Most ground samples have a Na^+/Cl^- ratio lower than 1.0, and close to the sea water relationship of 0.858 (Fig. 6a), and they are mostly in agreement with the mixing line between sea water and continental water contributions, the latest defined by the hydrochemical composition of Channel 2 at Site #3. The concurrence of the sodium and chloride values with the mixing line is due to the high solubility product of halite, which is considered as the main source of both elements. Specific deviations from the sea water equilibrium value, however, could be attributed to water–soil interaction, suggesting additional processes of chloride and sodium enrichment or depletion. In particular, a sample from the coastal plain at Site #2, and one sample from the sand sheet at Site #1 (Fig. 2), shows Na^+/Cl^- ratios of 2.0 and 1.7, respectively (Fig. 6a). These values also reflect an enrichment of sodium versus chloride, but also a depletion of $Ca^{2+} + Mg^{2+}$ versus $HCO_3^- + SO_4^{2-}$, suggesting a sodium–calcium exchange process in specific points of the subsurface, specifically those with a lesser influence of halite dissolu-

tion as indicated by the low chloride content of these samples (Fig. 7).

Sulphate also increases with chloride (Fig. 5b). Nevertheless, samples from all coastal plain monitoring wells, as well as those from the sand sheets, show a SO_4^{2-}/Cl^- ratio that differ from the theoretical mixing line (Fig. 6b). In that way, sulphate enrichment versus chloride is found in some samples from the coastal plain and the sand sheet at Sites #2 and #3, whereas sulphate depletion characterizes samples from sand sheets at Sites #1 and #2. Furthermore, the Ca^{2+}/SO_4^{2-} ratios of the ground water samples are usually distinct from those of sea water (0.364) showing a higher calcium concentration with respect to sulphate (Fig. 5c and Fig. 6c). Larger calcium content than the expected from a theoretical mixing line is found in most ground water samples, specifically in those with a sulphate concentration larger than 15 meq/L. Above this content, samples show a relationship between Ca^{2+} and SO_4^{2-} that approaches a ratio equal or larger than 1.0. Such a high Ca^{2+}/SO_4^{2-} ratio suggests underground gypsum dissolution, while the enrichment of calcium observed in some samples denotes a contribution from calcite dissolution.

Such hydrochemical composition, and the fact that the SO_4^{2-}/Cl^- and Ca^{2+}/SO_4^{2-} ratios are distinct of that of sea water, suggest that interaction with soil minerals is a governing factor that controls water salinity rather than a mixing process between the two mentioned end-members: sea water and mainland surface water as that from Channel 2.

Bicarbonate concentrations show a wide range of values, all of them higher than that of sea water (2.327 meq/L) (Table 1). Calcite saturation indexes are all above 0.0, showing oversaturation ratios even higher than the sea water saturation index for calcite (0.58) (Fig. 8a). Gypsum saturation indexes show a tendency towards oversaturation as the sulphate concentration increases (Fig. 8b). Such trend shows the usual distribution in fresh ground water environments (Plummer et al., 1990), where mineral saturation is gradually attained along the flow path as a function of water residence time within the aquifer. The highest gypsum saturation indexes in ground water samples mainly belong to most inland located samples in coastal plain and sand sheets deposits at Site #2 and #3. Halite saturation indexes are in general below the sea water value (−2.54), and halite saturation also increases proportionally to the chloride content (Fig. 8c). The evolution of halite saturation indexes shows a similar trend whether plotted against the chloride or the sulphate content (Fig. 8c and d). This points out that the progress towards saturation in both minerals depends on the hydrodynamic features of both deposits, in particular a large residence time due to the low hydraulic conductivity and hydraulic gradient in the underlying coastal plain deposits.

Among the major elements in solution, magnesium can be taken as representative of sea water occurrence at the subsurface, as it is seldom found with similar concentrations in ground water (Hem, 1985). In the study area, all contents are far below those of sea water (104.65 meq/L), ranging from 0.49 to 52.92 meq/L (Fig. 5d). Mg^{2+}/Cl^- ground water ratios are usually unrelated to the mixing line; although two samples from coastal plain locations at Site #2, and from sand sheet deposits at Site #3 show a ratio close to that of sea water (Fig. 6d). Major divergences from this ratio are due to the higher chloride content in samples from the coastal plain at Sites #1 and #2. Additional contribution of halite is, therefore, considered to be responsible for such high chloride concentrations, rather than effective sea water mixing by tidal processes that will provide a larger magnesium content in ground water. Concentration of salt water by transpiration can also explain the high concentrations in the residual soil water (Fass et al., 2007). Moreover, selective uptake of magnesium by plant roots in flooded saline areas is also known to create the necessary osmotic potential
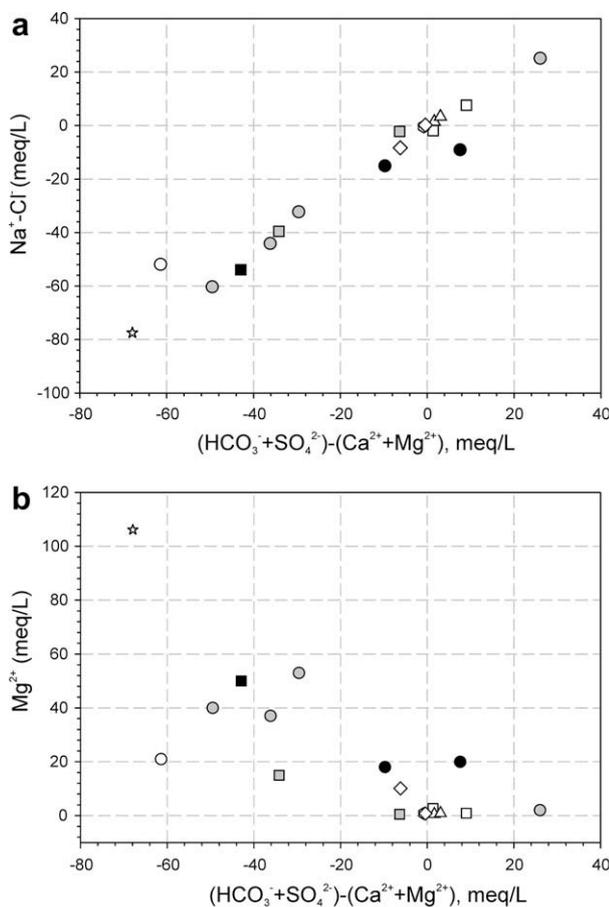

Fig. 7. Relationship between the calcite–gypsum and the halite poles as potential end-members in ground water hydrochemistry. Values with $(Na^+–Cl^-) > 0$, and $(HCO_3^- + SO_4^{2-}) − (Ca^{2+} + Mg^{2+}) > 0$ indicate efficient sodium–calcium exchange processes. Negative values of both factors are attributed to the balancing effect of magnesium in the water composition, as shown in the bottom graph. Legend as in Fig. 5.

to attract water and to expel other ions, as sodium, out of the root. This biological process will cause magnesium depletion and reduce the Mg^{2+}/Cl^- ratio.

Surface water hydrochemistry

In the study area, estuarine water from Río de la Plata shows salinity values of 15 g/L (Bazán and Arraga, 1993; Guerrero et al., 1997). The Ajó River presents chloride–sodium facies with varying salinity (1345–4345 mg/L) as a function of the contributions from the main tidal channel (El Palenque) and the inland freshwater channel (Channel 2) as governed by tidal oscillation (Table 1). In this way, surface water from the El Palenque tidal channel has chloride–sodium facies with salinity values ranging from 1495 to 7080 mg/L, this last value corresponding to the isotope sampling survey. Channel 2 waters vary in composition from chloride–sodium to bicarbonate–sodium facies, with low salinity values ranging from 575 to 1345 mg/L (Fig. 4).

In general, all surface waters present lower salinity content than most ground water samples (Table 1 and Fig. 5). Na^+/Cl^- ratios for the Ajó River and El Palenque channel waters are similar to that of sea water, and they lay close to the mixing line with sea water contributions estimated in less than 10% (Fig. 6a). Channel 2 presents a higher Na^+/Cl^w ratio, with an average value of 1.3, as a mark of the continental water characteristics. Furthermore, hydrochemical ratios of all surface waters are less than the sea water ratios, and they are mostly consistent with the mixing line indicating a minor tidal effect on surface waters (Fig. 6b–d).

Calcite saturation indexes of surface water samples, between 0.15 and 0.50, are below those of most of the ground water samples and the sea water reference value, with the sole exception of

a sample from Channel 2 (Fig. 8a). Similarly, all surface waters show gypsum and halite saturation indexes lower than those of sea water, and they all present a large degree of undersaturation (Fig. 8b and Fig. 8c).

Isotopes

Ground water

Coastal plain ground water samples show $\delta^{18}O$ values between −5.5 and −1.6‰, and δD values between −34‰ and −18‰ (Table 2, and Fig. 9). They all lie in the area bounded by evaporation lines with slopes of 4.0 and 5.2, corresponding to distinct values of atmospheric humidity (Gonfiantini, 1986; Gat, 1996; Clark and Fritz, 1997; Mazor, 1997). Evaporation line originates from averaged local rainfall values of $\delta^{18}O$ = −6.3‰, and δD = −40‰ (Panarello and Albero, 1983; Dapeña and Panarello, 2004). Both surface and ground water lay on an unique evaporation trend given by a regression equation of slope −4.89 (i.e., δD = −9.47–4.89 $\delta^{18}O$). Moreover, samples do not show any tendency towards standard isotopic sea water values (0.0‰, 0.0‰; Fig. 9).

Isotopic values of ground water samples from the coastal plain are related to the hydrological environments of the study sites. For instance, samples from Sites #1 and #2 lay on a neat evaporation line. Two of them show isotopical enrichment lower than that for surface waters, and a specific sample from Site #2 shows isotopic values close to those of the Ajó River. They denote distinct proportions from continental water sources, whether surface waters, coastal plain aquifer recharge, or local rainfall. A sample from the coastal plain at Site #3, however, approaches the local averaged rainfall isotopic value.
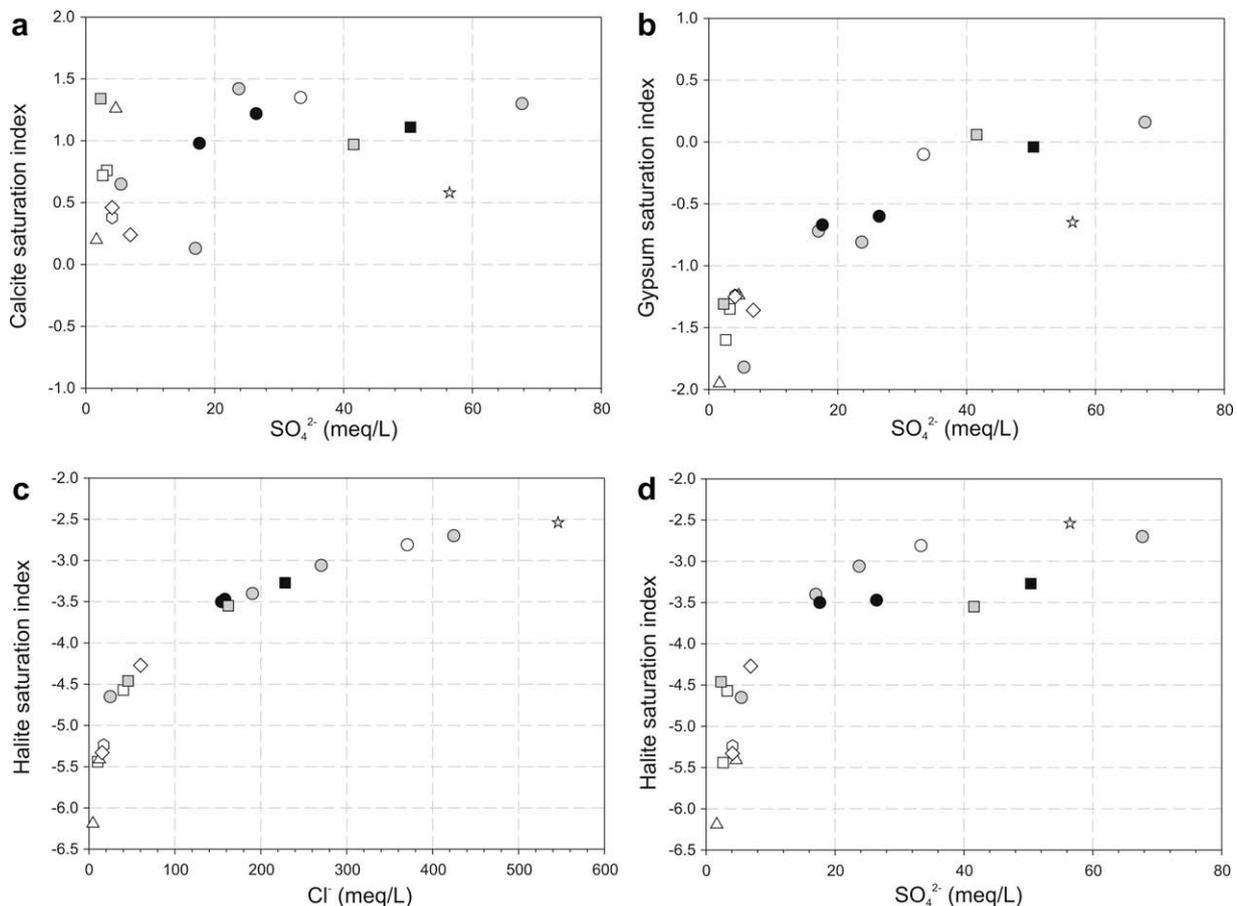

Fig. 8. Saturation indices of surface and ground water samples with increasing selected anion concentration. Saturation indices for sea water as estimated by Parkhurst and Appelo (1999). Legend as in Fig. 5.

Table 2
Isotopical data from surface and ground water.

	Sample	$\delta^{18}O$ ‰ (VSMOW)	δD ‰ (VSMOW)	d-Excess
Groundwater				
Coastal plain	CP1 S1	−3.9	−26	5.2
	CP3 S2	−1.6	−18	−5.2
	CP5 S2	−3.9	−28	3.2
	CP6 S3	−5.5	−34	10.0
Sand sheet	SS2 S1	−5.2	−39	2.6
	SS3 S2	−4.8	−35	3.4
	SS5 S3	−5.2	−35	6.6
Surface water				
Channel 2	C2 S2 HT	−2.9	−21	2.2
	C2 S2 LT	−2.8	−24	−1.6
	C2 S3 LT	−2.6	−21	−0.2
El Palenque	EP S2 HT	−0.3	−12	−9.6
channel	EP S2 LT	−0.4	−11	−7.8
	EP S3 LT	−0.7	−14	−8.4
Ajó River	R S1 HT	−0.9	−12	−4.8
	R S2 HT	−1.7	−17	−3.4
	R S2 LT	−1.4	−19	−7.8

S1, S2, and S3 in the sample name refer to Sites #1, #2, and #3, respectively. HT and LT indicate high tide and low tide.

Values of the d-excess factor (d-excess = $\delta D - 8\delta^{18}O$) around +5‰ indicates that ground water has undergone evaporation prior to infiltration (Fig. 9). In particular, samples from the coastal plain indicate a larger evaporation than those of the sand sheets; nevertheless, mixing with evaporated surface water should also be considered in the isotopical content of water samples from the coastal plain deposits.
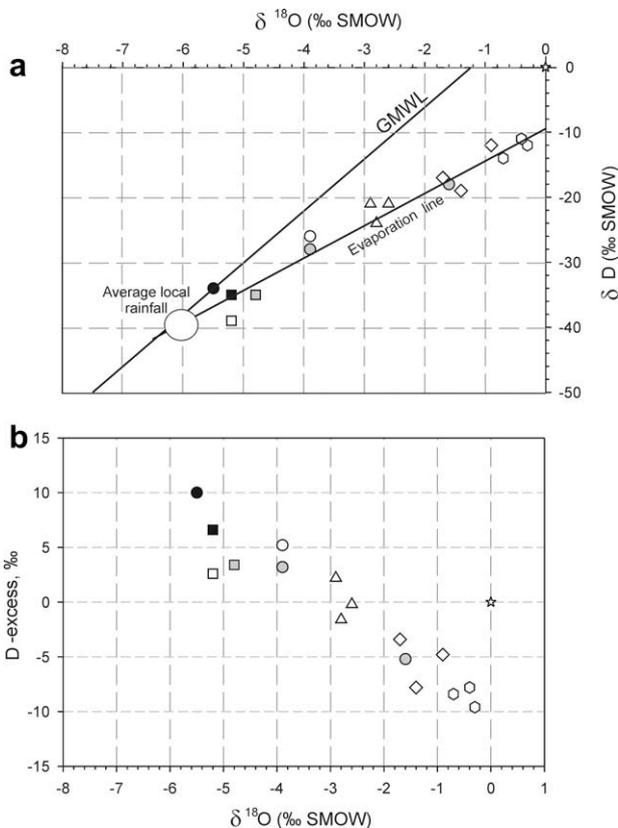

Fig. 9. Stable isotope relationship for surface and ground water samples and suggested evaporation trends in the area; and d-excess factor values with respect to $\delta^{18}O$, or to increasing evaporation rates. Legend as in Fig. 5.
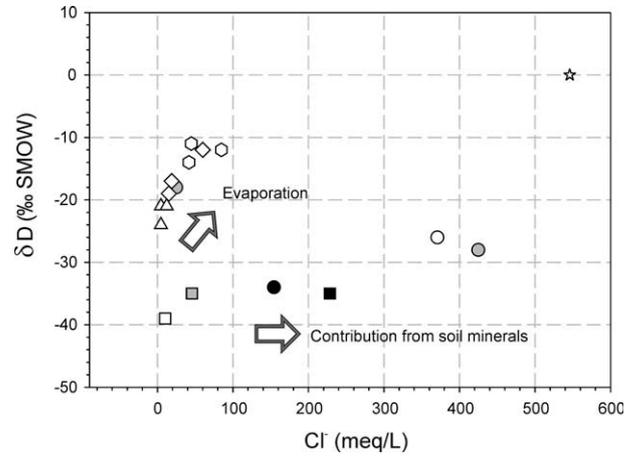

Fig. 10. Relationship between chloride content and isotopic signature of surface and ground water samples as a means to differentiate hydrogeological processes in the area.

Conversely, samples from the sand sheets show a lower level of enrichment, with isotopical values of $\delta^{18}O$ between −5.2‰ and −4.8‰, and of δD between −39‰ and −35‰ (Table 2, and Fig. 9). A low evaporation rate of the sand sheet ground water is consistent with its hydrodynamics which is determined by a high hydraulic conductivity, and therefore, faster infiltration rates, and a minor exposure of water in flooded areas by tidal oscillations. Moreover, the relationship between δD and the chloride content shows an increase in salinity at constant isotopical values of δD lower than −35‰ for the sand sheet ground water samples (Fig. 10), and with a slight increase up to $\delta D < -25$‰ for the coastal plain samples. This relationship between chemical and isotopical data is attributable to the contribution of gypsum and halite to ground water hydrochemistry, providing evidence of the non-participation of sea water as a significant source. The slight isotopic enrichment shown by the most saline waters is related to early evaporation processes (Gonfiantini and Araguás, 1988).

Surface water
Surface water samples are also located within the evaporation line shown in Fig. 9. No significant variations are observed between samples taken at high and low tides. The highest level of isotopical enrichment is observed in El Palenque waters with $\delta^{18}O$ values between −0.7‰ and −0.3‰, and δD values between −14‰ and −11‰. Additionally, samples from Channel 2 show lower values than those of El Palenque channel ($\delta^{18}O$ between −2.9‰ and −2.6‰, and δD between −24‰ and −21‰). Ajó River water at the junction between Channel 2 and El Palenque channels has an isotopic composition of $\delta^{18}O$ between −1.7‰ and −1.4‰, and δD between −19‰ and −17‰, indicating a significant mixing of both contributions. Ajó River surface water closer to the estuarine area shows an even heavier isotopical content of $\delta^{18}O = -0.9$‰, and $\delta D = -12$‰ (Table 2), but in line with evaporation trends and with no clear indication of sea water influence (Figs. 9 and 10). Indeed, surface waters, especially those of El Palenque channel related to the draining of the coastal plain under tidal influences, point out a large evaporation progress. In this case, surface waters show a joint increase in their chloride and δD contents, revealing the occurrence of evaporation processes from waters originally low in salinity (Fig. 10). These heavier isotopic values for surface water samples, their stability independently of the tide wave, and their relationship with isotopic ground water data, suggest a conceptual model in which surface water in tidal channels and coastal plain areas experience intense evaporation as reflected by their isotopical and chemical data.

Conclusions

Geomorphic units in Samborombón Bay, namely the coastal plain deposits and the aeolian sand sheets, play an important role in water resource distribution and its hydrological dynamics.

Coastal plain formations, related to a former tidal environment, present saline water of poor quality for human use. Nevertheless, hydrological ratios and isotopic values indicate a negligible contribution of sea water to these ground water resources. Rainfall recharge, jointly with an almost nil regional hydraulic gradient, results in a long residence time of water in the coastal plain shallow aquifer layers. Dissolution of gypsum and halite, as well as other chlorides, within the sedimentary formations and soil water is thus responsible for ground water salinity. Biological processes may influence metal concentration by transpiration and selective ion uptake. Present sea water from the Atlantic Ocean can not be considered as a true pole in the hydrological balance as water samples from tidal channels, specifically those from Ajó River, do not show a significant isotopical trend towards a marine water isotopic signature.

Ground water storage in the sand sheets constitutes the most valuable regional water resource, although its salinity may represent a constraint on some uses. Hydraulic dynamics, as well as salinity values, depend on the spatial variability of these aeolian deposits and their interbedding with the coastal plain sediments. Ground water resources in the sand sheets are restricted by the fact they are not very thick (usually a few metres), and monthly rainfall distribution and intensity.

The current water demand for human uses, including domestic, agricultural and cattle rearing needs, is provided by Channel 2, and ground water withdrawal from sand sheets. Evidence of ground water salinization processes highlights the weaknesses of this hydrological system. Therefore, further urban and/or industrial development of the area, or tourist resorts, would require a balance between water availability and human demand so that ecological integrity could be guaranteed together with economic vitality in a sustainable framework of water management.

References

Ainchil, J., Calahorra Fuertes, P., Kruse, E., 2004. Variaciones químicas del flujo subterráneo en la planicie costera próxima a La Plata, Argentina. In: Proceedings: Groundwater Flow Understanding: XXXIII Congress IAH – 7° Congress Alhsud, T2-31, Zacatecas (México).

APHA (American Public Health Association). 1998. Standard Methods for the Examination of Water and Wastewater, 20th ed. American Public Health Association, American Water Works Association, Water Environment Federation, Washington, DC.

Bazán, J., Arraga, E., 1993. Rio de la Plata ¿Un sistema fluvio marítimo frágil? Acercamiento a una definición de la calidad de sus aguas. In: Boltovskoy, A., López, H. (Eds.), Conferencia de Limnología, pp. 71–82.

Carol, E., 2008. Procesos hidrológicos en el sector sur de la Bahía de Samborombón. Tesis doctoral, Universidad Nacional de La Plata, 236.

Carol, E., Kruse, E., Pousa, J., 2008. Environmental hydrogeology of the southern sector of the Samborombón bay wetland, Argentina. Environmental Geology 54, 95–102.

Clark, I., Fritz, P., 1997. Environmental Isotopes in Hydrology. CRC Press, Boca Raton, FL.

Coleman, M., Sheperd, T., Durham, J., Rouse, J., Moore, F., 1982. A rapid and precise technique for reduction of water with zinc for hydrogen isotope analysis. Analytical Chemistry 54, 993–995.

Dapeña, C., Panarello, H., 2004. Composición isotópica de la lluvia de Buenos Aires. Su importancia para el estudio de los sistemas hidrológicos pampeanos. Revista Latino-Americana de Hidrogeología 4, 17–25.

Djabri, L., Rouabhia, A., Hani, A., Lamouroux, Ch., Pulido-Bosch, A., 2008. Origin of water salinity in a lake and coastal aquifer system. Environmental Geology 54, 565–573.

El Mandour, A., El Yaouti, F., Fakir, Y., Zarhloule, Y., Benavente, J., 2008. Evolution of groundwater salinity in the unconfined aquifer of Bou-Areg, Northeastern Mediterranean coast, Morocco. Environmental Geology 54, 491–503.

Fass, T., Cook, P.G., Stieglitz, T., Herczeg, A.L., 2007. Development of saline ground water through transpiration of sea water. Ground Water 45, 703–710.

Gat, J.R., 1996. Oxygen and hydrogen isotopes in the hydrologic cycle. Annual Review of Earth and Planetary Science 24, 225–262.

Ghabayen, S., McKee, M., Kemblowski, M., 2006. Ionic and isotopic ratios for identification of salinity sources and missing data in the Gaza aquifer. Journal of Hydrology 318, 360–373.

Gonfiantini, R., 1978. Standard for stable isotope measurements in natural compounds. Nature, 271–534.

Gonfiantini, R., 1986. Environmental isotopes in lake studies. In: Fritz, P., Fontes, J.C. (Eds.), Handbook of Environmental Isotope Geochemistry. Elsevier, pp. 113–168.

Gonfiantini, R., Araguás, L., 1988. Los isótopos ambientales enel estudio de la intrusión marina. Simposio Internacional Tecnología de la Intrusión en Acuíferos Costeros, Instituto Geológico y Minero de España, pp. 135–190.

Groen, J., Velstra, J., Meesters, A., 2000. Salinization processes in paleowaters in coastal sediments of Suriname: evidence from $\delta^{37}Cl$ analysis and diffusion modelling. Journal of Hydrology 234, 1–20.

Guerrero, R., Acha, E., Framiñan, M., Lasta, C., 1997. Physical oceanography of the Rio de la Plata Estuary, Argentina. Continental Shelf Research 17, 727–742.

Hem, J.D., 1985. Study and interpretation of the chemical characteristics of natural water. US Geological Survey Water Supply Paper 2254, 263 pp.

Howard, K., Lloyd, J., 1983. Major ion characterization of coastal saline ground waters. Ground Water 21, 429–437.

Jorgensen, N., 2002. Origin of shallow saline groundwater on the Island of Laeso, Denmark. Chemical Geology 184, 359–370.

Kamel, S., Dassi, L., Zouari, K., Abidi, B., 2005. Geochemical and isotopic investigation of the aquifer system in the Djerid-Nefzaoua basin, southern Tunisia. Environmental Geology 49, 159–170.

Kim, Y., Lee, K., Koh, D., Lee, D., Lee, S., Park, W., Koh, G., Woo, N., 2003. Hydrogeochemical and isotopic evidence of groundwater salinization in a coastal aquifer: a case study in Jeju volcanic island, Korea. Journal of Hydrology 270, 282–294.

Kruse, E., Laurencena, P., Varela, L., Rojo, A., Deluchi, M., 2005. Hydrological characterization of the brackish – fresh water relationship in different morphological environments of the province of Buenos Aires, Argentina. Geological Survey of Spain: Series on Hydrogeology and Groundwater 15, 305–312.

Logan, W., Rudolph, D., 1997. Microdepressión-focused recharge in a coastal wetland, La Plata, Argentina. Journal of Hydrology 194, 221–238.

Logan, W., Nicholson, R., 1998. Origin of dissolved groundwater sulphate in coastal plain sediments of the Rio de la Plata, Eastern Argentina. Aquatic-Geochemistry 3, 305–328.

Logan, W., Auge, M., Panarello, H., 1999. Bicarbonate, sulfate and chloride water in a shallow, clastic-dominated coastal flow system, Argentina. Ground Water 37, 287–295.

Marimuthu, S., Reynolds, D., Le Gal La Salle, C., 2005. A field study of hydraulic, geochemical and stable isotope relationships in a coastal wetlands system. Journal of Hydrology 315, 93–116.

Mazor, E., 1997. Chemical and Isotopic Groundwater Hydrology: The Applied Approach. Marcel Dekker, New York. p. 413.

Panarello, H., Albero, M., 1983. Tritium, oxygen-18 and deuterium contents of Buenos Aires rainwater. Coloquio Internacional de Grandes Llanuras II, 889–898.

Panarello, H., Paricia, C., 1984. Isótopos del oxígeno en hidrogeología e hidrología. Primeros valores en agua de lluvia de Buenos Aires. Revista de la Asociación Geológica Argentina 34, 3–11.

Park, S., Yun, S., Chae, G., Yoo, I., Shin, K., Heo, C., Lee, S., 2005. Regional hydrochemical study on salinization of coastal aquifers, western coastal area of South Korea. Journal of Hydrology 313, 182–194.

Parker, G., 1979. Geología de la planicie costera entre Pinamar y Mar de Ajó, provincia de Buenos Aires. Revista de la Asociación Geológica Argentina 34, 167–183.

Parkhurst, D.L., Appelo, C.A.J., 1999. User's guide to PHREEQC (Version 2). A computer program for speciation, batch-reaction, one-dimensional transport, and inverse geochemical calculations: US Geological Survey Water-Resources Investigations Report 99-4259, 310 p.

Plummer, N., Busby, J., Lee, R., Hanshaw, B., 1990. Geochemical modeling of the Madison aquifer in parts of Montana, Wyoming, and South Dakota. Water Resources Research 26, 1981–2014.

Robinson, B., Gunatilaka, A., 1991. Stable isotope studies of the hydrological regime of Sabhas in southern Kuwai, Arabian Gulf. Sedimentary Geology 73, 141–159.

Sala, J., González, N., Hernández, M., 1978. Efectos de una barrera hidráulica natural en las aguas subterráneas del litoral de la Bahía de Samborombón. Obra del Centenario del Museo de La Plata, Tomo IV, 153–166.

Soil Taxonomy, 1999. A Basic System of Soil Classification for Working and Interpreting Soil Surveys, second ed. United States Government Printing Office, Washington.

Stumm, W., Morgan, J., 1981. Aquatic Chemistry, second ed. Wiley. P. 780.

Thornthwaite, C., 1948. An approach toward a rational classification of climate. Geographical Review 38, 55–94.

Thornthwaite, C., Mather, J., 1955. The water balance, 8. Drexel Institute of Technology, Laboratory of Climatology, Certerton, N.J. pp. 1–104.

Violante, R., Parker, G., 2000. El Holoceno en las regiones marinas y costeras del noreste de la Provincia de Buenos Aires. Revista de la Asociación Geológica Argentina 55, 337–351.

Violante, R., Parker, G., Cavallotto, J., 2001. Evolución de las llanuras costeras del este bonaerense entre la bahía de Samborombón y la laguna de Mar Chiquita durante el Holoceno. Revista de la Asociación Geológica Argentina 56, 51–66.